

ON THE DYNAMICS OF SUDDENLY HEATED ACCRETION DISKS AROUND NEUTRON STARS

D. R. BALLANTYNE AND J. E. EVERETT

Canadian Institute for Theoretical Astrophysics, McLennan Labs, 60 St. George Street, Toronto,
ON M5S 3H8, Canada; ballantyne@cita.utoronto.ca, everett@cita.utoronto.ca

Received 2004 December 8; accepted 2005 February 17

ABSTRACT

Type I X-ray bursts and superbursts on neutron stars release sudden and intense radiation fields into their surroundings. Here we consider the possible effects of these powerful explosions on the structure of the accretion disk. The goal is to account for the apparent evolution of the innermost regions of the accretion disk around 4U 1820–30 during a superburst. Three different processes are considered in detail: radiatively or thermally driven outflows, inflow due to Poynting-Robertson drag, and a structural change to the disk by X-ray heating. Radiatively driven winds with large column densities can be launched from the inner disk, but only for $L/L_{\text{Edd}} \gtrsim 1$, which is expected to be obtained only at the onset of the burst. Furthermore, the predicted mass outflow rate is less than the accretion rate in 4U 1820–30. Estimates of the Poynting-Robertson or radiative drag timescale show that it is a very efficient means of removing angular momentum from the gas. However, the analytical results are likely only applicable at the innermost edge of the disk. X-ray heating gives a change in the disk scale height that is correlated with the blackbody temperature, as seen in the evolution during the 4U 1820–30 superburst. If this change in the scale height can alter the surface density, then the viscous time (with $\alpha \sim 0.03\text{--}0.2$) is the closest match to the 4U 1820–30 results. We expect, however, that all three processes are likely ongoing when an accretion disk is subject to a sudden heating event. Ultimately, a numerical simulation of a disk around a bursting neutron star is required to determine the exact response of the disk. Magnetic truncation of the accretion flow is also considered and applied to the 4U 1820–30 X-ray reflection results.

Subject headings: accretion, accretion disks — radiation mechanisms: thermal — stars: individual (4U 1820–30) — stars: neutron — X-rays: bursts

1. INTRODUCTION

Accretion disks around neutron stars are often subject to sudden intense radiation fields due to type I X-ray bursts (Lewin et al. 1993, 1995; Bildsten 1998; Strohmayer & Bildsten 2005; Cumming 2004), or, on rare occasions, superbursts (Cornelisse et al. 2000; Cumming & Bildsten 2001; Strohmayer & Brown 2002; Kuulkers 2004). These events can reach the Eddington luminosity and thus deposit a large amount of energy in the accretion disk over a short amount of time (tens of seconds for type I bursts; hours for superbursts). The accretion disk structure may be altered by this sudden injection of energy, as suggested by the evolution of X-ray reflection features observed from the low-mass X-ray binary (LMXB) 4U 1820–30 during a superburst (Ballantyne & Strohmayer 2004). In this source, modeling of Fe $K\alpha$ line and edge features produced by the disk indicated that the reflecting part of the disk moved outward from $\sim 20r_g$ ($r_g = GM/c^2$, where M is the mass of the neutron star) to $\sim 100r_g$ in ~ 1000 s before eventually returning to $\sim 10r_g$. This behavior was puzzling, because the change in the reflecting radius was not correlated with the observed X-ray flux but with the hardness of the blackbody spectrum. Ballantyne & Strohmayer (2004) therefore proposed a model in which the surface density of the inner accretion disk was altered by heating from the incident X-rays; however, alternative models have not yet been carefully considered.

In this paper, we examine in detail a number of different physical processes that may alter the structure of accretion disks during a sudden heating event. The physics are treated as generally as possible, but quantitative comparisons are made with the 4U 1820–30 results in order to test the individual models as possible explanations for the inferred behavior.

We begin in § 2 by reviewing the observed properties of 4U 1820–30. The paper is then broken into three sections based on the different possibilities for the accretion disk response. In § 3 we consider outflow mechanisms, such as thermally and radiatively driven winds. Section 4 contains a study of inflow onto the central object via radiative drag. Changes to the disk structure that do not involve inflow or outflow are the subject of § 5. The results are gathered and discussed in § 6. Finally, conclusions are drawn in § 7.

2. OVERVIEW OF 4U 1820–30

With an orbital period of only 11.4 minutes, 4U 1820–30 is one of the most compact LMXBs known (Stella et al. 1987). Evolutionary models of the system (Verbunt 1987; Bailyn & Grindlay 1987; Rappaport et al. 1987; Rasio et al. 2000) all predict that the accreting material is primarily helium. Type I X-ray bursts from 4U 1820–30 have been observed for nearly 30 years (Grindlay et al. 1976; Haberl et al. 1987; Kuulkers et al. 2003) and have recurrence times between 2 and 4 hr. Cumming (2003) presents further details and models of the type I X-ray bursts from 4U 1820–30.

Although the system resides within the metal-rich globular cluster NGC 6624, the distance to 4U 1820–30 is still not precisely known. The difficulty arises because of uncertainties in the interstellar extinction along the line of sight and in the metallicity relation used to correct the absolute magnitude of horizontal branch stars. Thus, using the same technique, Kuulkers et al. (2003) derived the distance to 4U 1820–30 of 7.6 ± 0.4 kpc, in agreement with an earlier estimate (Rich et al. 1993), while Vacca et al. (1986) found it to be 6.4 ± 0.6 kpc. Most recently, Shaposhnikov & Titarchuk (2004) modeled the light curve and

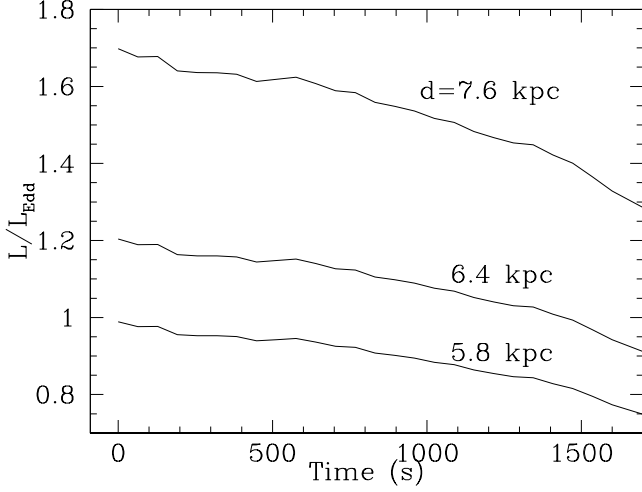


FIG. 1.—Time evolution of L/L_{Edd} during the first ~ 1700 s of the 4U 1820–30 superburst. The three curves show the results for different distance estimates to the system. The value for L_{Edd} is taken to be 2.7×10^{38} ergs s^{-1} , assuming a canonical neutron star ($M = 1.4 M_{\odot}$, $R = 10$ km) with a helium atmosphere. The observed luminosity was calculated between 0.1–40 keV using the best-fitting spectral models of Ballantyne & Strohmayer (2004) and assuming isotropic radiation.

spectrum of a photospheric radius expansion (PRE) burst from 4U 1820–30 and determined a distance of ~ 5.8 kpc.

The Eddington luminosity at the photosphere of a neutron star with a helium atmosphere, as determined by a distant observer, is

$$L_{\text{Edd}} = 2.5 \times 10^{38} \left(\frac{M}{M_{\odot}} \right) \times \left[1 - 0.295 \left(\frac{M}{M_{\odot}} \right) \left(\frac{R_{*}}{10 \text{ km}} \right)^{-1} \right]^{1/2} \text{ ergs s}^{-1}, \quad (1)$$

where R_{*} is the radius of the photosphere (Lewin et al. 1993). Employing the standard assumptions (which will be made throughout this paper) of a $1.4 M_{\odot}$, 10 km radius neutron star, $L_{\text{Edd}} = 2.7 \times 10^{38}$ ergs s^{-1} . In Figure 1 we plot the time evolution of L/L_{Edd} over the first 1600 s of the 4U 1820–30 superburst. The observed luminosity was calculated by measuring the 0.1–40 keV flux predicted from the best-fitting spectral models of Ballantyne & Strohmayer (2004) and assuming isotropic radiation. Separate curves are plotted for the different distance estimates described above. Since large super-Eddington luminosities are not expected for X-ray bursts (e.g., Joss & Melia 1987), this figure seems to indicate that the 5.8 kpc distance may be the most reasonable. However, by using equation (1) we find that increasing the mass and radius of the neutron star to, for example, $1.7 M_{\odot}$ and 12 km, respectively, would make the 6.4 kpc distance consistent with L_{Edd} . The 7.6 kpc distance is more challenging, but a much larger mass and radius (for example, $M = 2.3 M_{\odot}$ and $R = 18$ km) can allow the Eddington luminosity to approach the observed value. Such a large mass is implied by the highest frequency of the kilohertz quasi-periodic oscillation (QPO) discovered from 4U 1820–30 if it is assumed to correspond to the orbital frequency at the innermost stable circular orbit (Zhang et al. 1998). Finally, it is worth noting that since the superburst had a PRE phase to it, the emitting photosphere may be larger than the true stellar radius, resulting in L_{Edd} being underestimated and therefore overestimating L/L_{Edd} . Because of

these uncertainties, we will, if necessary, use all three values of the distance in the following sections and continue to assume $L_{\text{Edd}} = 2.7 \times 10^{38}$ ergs s^{-1} .

X-ray bursts are seen from 4U 1820–30 when the persistent X-ray flux is $\lesssim 4 \times 10^{-9}$ ergs $\text{cm}^{-2} \text{s}^{-1}$, which is the low end of the observed range. This emission is powered by accretion onto the neutron star, so the flux can be converted to an accretion rate, $\dot{M} \approx 1.1 \times 10^{17} (d/6.4 \text{ kpc})^2 \text{ g s}^{-1} = 1.7 \times 10^{-9} (d/6.4 \text{ kpc})^2 M_{\odot} \text{ yr}^{-1}$ (Strohmayer & Brown 2002), consistent with the prediction of gravitational radiation driven mass loss (Stella et al. 1987). Using the above value of L_{Edd} and the observed persistent luminosity, we obtain an Eddington fraction of $M/\dot{M}_{\text{Edd}} = 0.07 (d/6.4 \text{ kpc})^2$, where $\dot{M}_{\text{Edd}} = L_{\text{Edd}}/\eta c^2$ is the Eddington mass accretion rate (η is the accretion efficiency).

3. OUTFLOWS

3.1. Radiatively Driven Winds

Type I X-ray bursts and superbursts may sometimes reach the Eddington luminosity L_{Edd} , as witnessed in the radiation expansion phase, where the photosphere of the burning material can be lifted off of the neutron star (e.g., Lewin et al. 1984; Strohmayer & Bildsten 2005). At these luminosities the momentum in the radiation field may also affect the inner regions of the accretion disk, possibly even blowing it away from the central object. Below, we check whether a radiatively driven wind can explain the behavior of 4U 1820–30 during the superburst.

3.1.1. Estimates from Accretion Disk Theory

Before diving into the models of radiative winds, it is worth calculating some simple estimates of outflow rates and energetics from basic Shakura & Sunyaev (1973) accretion disk theory to compare against the computations.

The X-ray modeling showed that the reflecting region moved from $\sim 20r_g$ to $\sim 100r_g$ in 500–1000 s (Ballantyne & Strohmayer 2004). It is unknown what occurred to the material within $20r_g$ to prevent it from reflecting (this is speculated upon in § 6), so we will only consider the evolution of the disk between $20r_g$ and $100r_g$. The accretion rate onto the neutron star is low enough (for all three values of the distance) that almost all of the radiation pressure dominated region of the disk will be within $20r_g$ (Shakura & Sunyaev 1973); thus, we will work only with the equations for a gas-supported disk with electron-scattering opacity. In this domain, the surface density of the disk can be written as

$$\Sigma = 2.5 \times 10^{13} (\mu m_p)^{4/5} [0.2(1 + X)]^{-1/5} \alpha^{-4/5} \times \left(\frac{M}{M_{\odot}} \right)^{-2/5} \dot{M}^{3/5} \left(\frac{R}{r_g} \right)^{-3/5} J(R)^{3/5} \text{ g cm}^{-2}, \quad (2)$$

where R is the radius along the disk, μ is the mean molecular weight of the accreting gas, m_p is the proton mass, X is the mass fraction of hydrogen, α is the Shakura-Sunyaev viscosity parameter, and $J(R) = [1 - (6r_g/R)^{1/2}]$ (e.g., Svensson & Zdziarski 1994). For 4U 1820–30, $\dot{M} \approx 1.1 \times 10^{17} (d/6.4 \text{ kpc})^2 \text{ g s}^{-1}$, $X \approx 0$, and $\mu \approx 1.3$ for a fully ionized gas with a cosmic abundance of heavy metals. This results in

$$\Sigma = 6 \times 10^4 \alpha^{-4/5} \left(\frac{M}{1.4 M_{\odot}} \right)^{-2/5} \left(\frac{\dot{M}}{1.1 \times 10^{17} \text{ g s}^{-1}} \right)^{3/5} \times \left(\frac{d}{6.4 \text{ kpc}} \right)^{6/5} \left(\frac{R}{r_g} \right)^{-3/5} J(R)^{3/5} \text{ g cm}^{-2}. \quad (3)$$

We then integrate equation (3) between $20r_g$ and $100r_g$ to estimate the total mass in the disk that needs to be removed by an outflow, $m = 3.2 \times 10^{19} (d/6.4 \text{ kpc})^{6/5} \text{ g}$, where we have assumed $\alpha = 0.1$. If this mass is removed in $\sim 500 \text{ s}$, then we obtain a mean mass outflow rate of $\dot{m} = 6.4 \times 10^{16} (d/6.4 \text{ kpc})^{6/5} \text{ g s}^{-1}$. This is the same order of magnitude as the accretion rate onto the neutron star, which implies that an even higher outflow rate is needed in order to remove the inner disk.

If this material is initially being lifted off an area A of the disk at the sound speed c_s , then by mass continuity, $\dot{m} = \rho c_s A = \bar{n} m_{\text{He}} c_s A$, where \bar{n} is the mean number density of helium at the disk surface. Writing the sound speed as $c_s = (kT/\mu m_p)^{1/2}$ and taking $kT = 2.6 \text{ keV}$, the temperature of the blackbody near the beginning of the superburst (Strohmayer & Brown 2002), gives $c_s \approx 435 \text{ km s}^{-1}$. If the launching area is an annulus between $20r_g$ and $100r_g$, then $\bar{n} = 1.7 \times 10^{17} (d/6.4 \text{ kpc})^{6/5} \text{ cm}^{-3}$. This is much lower than the number density predicted by Shakura & Sunyaev (1973) but may be reasonable for the surface layers at which the density must fall off rapidly.

Equation (3) can also be used to calculate the gravitational potential energy of the disk material between $20r_g$ and $100r_g$, $5.2 \times 10^{38} (d/6.4 \text{ kpc})^{16/5} \text{ ergs}$. The energy released during the first $\sim 1500 \text{ s}$ of the 4U 1820–30 superburst is $10^{41}–10^{42} \text{ ergs}$, assuming isotropic radiation. Therefore, there seems to be enough energy in the radiation field to completely remove the reflecting region of the accretion disk in a radiatively driven wind. The viability of such a wind is considered in more detail below.

3.1.2. Numerical Models

A numerical wind model can be used to calculate the radiative acceleration, velocity, and escape time for outflowing gas. For this paper, we define a model of a continuum-driven wind, launched from the accretion disk and moving along radial streamlines (radial because the wind is driven by momentum taken from radially streaming photons). This outflow structure therefore fills an open bi-cone in which gas flows radially outward, nearly along the surface of the accretion disk (for simplicity, the wind is set here to flow at a constant 5° above the disk).

The wind's acceleration is computed by taking the local velocity, density, ionization structure, and transmitted continuum into account. The outflow is launched from a user-defined radius with a nearly optically thick column at the disk (the maximum column that radiation driving could support), with the initial outflow speed set to the sound speed. The photoionization of this outflowing gas is then simulated using CLOUDY (Ferland 2002) at various heights in the wind. These simulations yield both the transmitted continuum and the ionization state of the gas from which the radiative acceleration can be calculated. Integrating this acceleration then yields the solution for the velocity as a function of distance along the wind. We then iterate on this solution to ensure that the density, photoionization, acceleration, and velocity profiles are all consistent.¹

The initial conditions for the model are chosen to match the observed and modeled properties of 4U 1820–30 (Strohmayer & Brown 2002; Ballantyne & Strohmayer 2004). First, the gas is illuminated with a 2.6 keV blackbody continuum, matching the temperature inferred by Strohmayer & Brown (2002) near the peak of the observed flux. We use gas abundances for cool

¹ This model follows largely the same method as presented in Everett & Ballantyne (2004). In contrast to that earlier work, however, the angular momentum of the orbiting gas in these simulations is set solely by the mass of the central object (since the initial angular momentum was set by the quiescent luminosity, not the outburst luminosity modeled here).

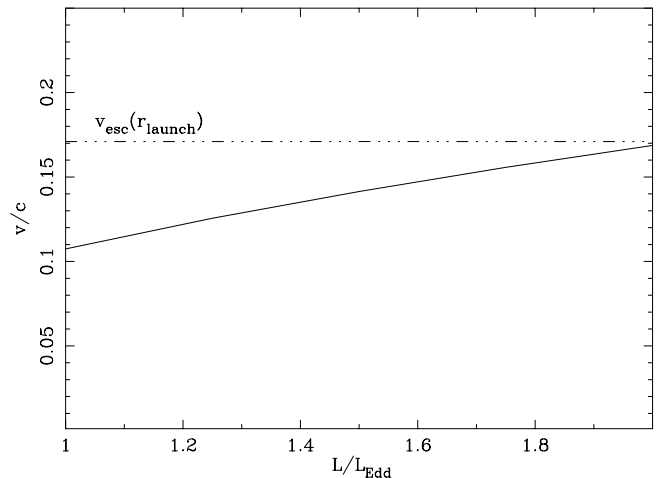


FIG. 2.—Final velocity of a continuum-driven wind with column density $N_{\text{H}} = 10^{24} \text{ cm}^{-2}$ as a function of the Eddington ratio. The escape velocity for $r_{\text{launch}} \sim 70r_g = 1.4 \times 10^7 \text{ cm}$ is given with the triple-dot-dashed line.

extreme helium stars as given by Pandey et al. (2001). The initial number density was set to 10^{17} cm^{-3} at the disk's surface, as implied by the simple calculation in § 3.1.1.² The innermost streamline of the wind is set to a radius of $20r_g$, the initial distance derived from the Fe K α line. As mentioned above, the base of the wind is simulated as being approximately optically thick with $N_{\text{H}} = 10^{24} \text{ cm}^{-2}$ to model the entire wind that would be launched radiatively from the disk and to set a conservative limit on the velocity of the outflowing gas. At the specified initial density, this column implies wind-launching radii of $20r_g$ to $\sim 70r_g$, approximately the same range as the observed variation in the Fe K α emission radius. These models are then run for a range of L/L_{Edd} values. For these calculations, it is important to note that the L_{Edd} defined in § 2 is replaced by the local Eddington luminosity for the accretion disk gas at $r \gtrsim 50r_g$, where relativistic effects are not important. At those distances, we can effectively disregard the final bracketed expression in equation (1), yielding $L_{\text{Edd}} = 3.5 \times 10^{38} \text{ ergs s}^{-1}$. Thus, L/L_{Edd} is set to the local value that the disk and wind would see.

With the above parameters, models are then run for a range of Eddington ratios to examine the resultant outflow velocities. These simulations show that the gas is highly ionized by the superburst, such that the wind is accelerated only by electron scattering and bound-free opacity of the wind, justifying a posteriori the approximation that the wind is continuum-driven. Figure 2 shows the velocity of this wind at $\sim 100r_g$ as a function of the Eddington ratio.

The time required for the gas to be launched from $20r_g$ to $100r_g$ is calculated by a numerical integral over $dr/v(s)$, where $v(s)$ is the velocity as a function of distance along the outflow streamline. The results are shown in Figure 3 for the model in which $N_{\text{H}} = 10^{24} \text{ cm}^{-2}$ at the base of the wind. The gas would easily be driven beyond $100r_g$ in much less than $\sim 500–1000 \text{ s}$ as long as the source has $L/L_{\text{Edd}} \gtrsim 1$. These results are insensitive to changes in initial conditions, such as the initial density or blackbody temperature, since variations in either do not

² Our assumed base density is much greater than the 10^{13} cm^{-3} limit beyond which CLOUDY's three-body recombination calculations are defined (Ferland 2002). However, for these luminosities, the ionization level is so high ($U = n_{\text{ion}}/n_{\text{He}} \sim 10^{4.5}$, where n_{ion} is the density of ionizing photons) that this will not substantially affect our results.

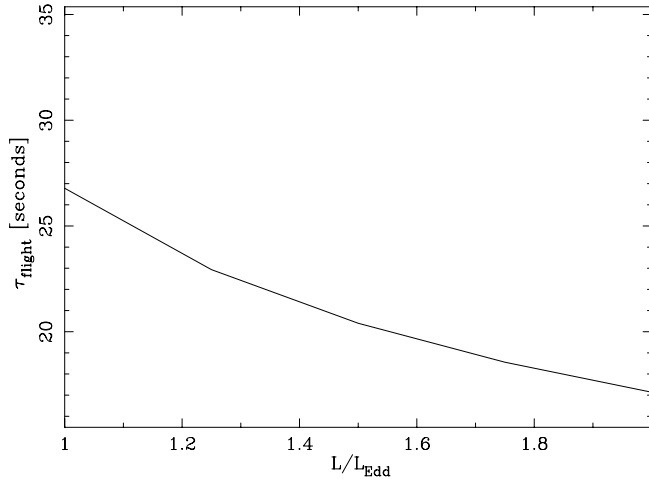


FIG. 3.—Time of flight for gas launched at $\sim 20r_g$ to reach $100r_g$ from the central source.

substantially change the ionization state of the gas or the continuum acceleration.

We now ask whether the mass outflow rate from the disk is enough to remove a significant amount of mass from the accretion disk. From the above model with $n_{\text{He}} = 10^{17} \text{ cm}^{-3}$ for $L/L_{\text{Edd}} \sim 1$, $v \sim 0.11c$ and $n_{\text{wind}} \sim 1.9 \times 10^{14} \text{ cm}^{-3}$ at $r = 100r_g = 2.07 \times 10^7 \text{ cm}$. Calculating $\dot{m}_{\text{out}} = 4\pi r^2 f \rho v$, where f is the covering fraction of the outflow, we find $\dot{m}_{\text{out}} \sim 2.3 \times 10^{16} f \text{ g s}^{-1}$. In § 3.1.1 we estimated from standard accretion theory that an outflow rate of $\sim 6 \times 10^{16} \text{ g s}^{-1}$ would be required to remove the inner part of the disk. The geometry of the calculated streamlines imply $f \sim 0.1$, resulting in an outflow rate ~ 30 times smaller than the theoretical estimate. Therefore, these calculations show that it is feasible for a continuum-driven outflow to remove a significant portion of the inner accretion disk during a superburst, but only for $L/L_{\text{Edd}} \gtrsim 1$, and it would not completely empty the inner accretion disk around 4U 1820–30 on the timescales observed ($\sim 500 \text{ s}$). The observed mass accretion rate for this system is $1.1 \times 10^{17} \text{ g s}^{-1} (d/6.4 \text{ kpc})^2$ (§ 2), implying that the replenishment rate in the disk is very competitive with the outflow rate.

3.2. Thermally Driven Winds

The gas near the surface of the accretion disk around the neutron star will be subject to intense X-ray heating by the explosion. If the temperature of the material increases to the point at which the local sound speed exceeds the escape velocity, then a thermal, pressure-driven wind could form, removing material from the disk. This mechanism has been proposed as a means to disperse circumstellar gas around newly forming stars (e.g., Font et al. 2004). However, it is very unlikely that such a wind will form close to a compact object such as a neutron star, where the escape velocity will be a large fraction of the speed of light. This can be seen explicitly by comparing the temperature of the irradiated gas to the virial temperature $kT_v \sim GM\mu m_p/R$. During an outburst by the central source, the temperature at the accretion disk surface will be dominated by photoionization, so it will maximize at the Compton temperature. For the case of 4U 1820–30, the peak temperature of the illuminating blackbody was $\sim 3 \text{ keV}$ (Strohmayer & Brown 2002), which will also be the value of the Compton temperature of the illuminated gas (§ 5). For gas with $\mu \approx 1.3$ orbiting a $1.4 M_{\odot}$ neutron star at $20r_g$, $kT_v \sim 6 \times 10^4 \text{ keV}$. Clearly, thermal pressure alone will not cause

the heated gas to flow from the system. Other forces are required to overcome the strong gravity of the neutron star and cause gas to outflow (§ 3.1).

4. INFLOW

X-ray photons produced in the explosion on the surface of the neutron star can remove angular momentum from the accretion flow by Poynting-Robertson drag (Poynting 1903; Robertson 1937; Blumenthal 1974). This will increase the local accretion rate and potentially could drain material from the inner part of the disk inward and onto the star (Walker & Mészáros 1989; Walker 1992; Miller & Lamb 1993, 1996). If this effect operates efficiently, it may provide another possible explanation for the apparent accretion disk evolution observed in 4U 1820–30.

A simple estimate of the mass affected by radiation drag is when it interacts with its own rest mass of light, $M_{\text{PR}} \sim Lt/c^2$, where t is the duration of the event (e.g., Walker & Mészáros 1989). In the case of 4U 1820–30, $Lt \sim 10^{41} - 10^{42} \text{ ergs}$ (§ 3.1.1), which gives $M_{\text{PR}} \sim [1.1 \times (10^{20} - 10^{21})] f \text{ g}$, where f is the fraction of the luminosity intercepted by the disk. Even if $f \sim 0.1$, this estimate is comparable to the mass in the affected region of the accretion disk (§ 3.1.1). We now check the timescale for angular momentum loss.

For circular orbits with velocity v_{ϕ} , the rate of change of angular momentum, l , is related to the change of radius r by

$$\frac{1}{l} \frac{dl}{dt} = \frac{1}{2r} \frac{dr}{dt}. \quad (4)$$

The theory of Poynting-Robertson drag gives the angular momentum loss rate as a function of the source luminosity L and r (e.g., Blumenthal 1974):

$$\frac{dl}{dt} = \frac{-\sigma_T \beta L \zeta w}{4\pi cr} \mathcal{E}, \quad (5)$$

where σ_T is the Thomson cross section, $\beta = v_{\phi}/c$, ζ is the mean number of scattering electrons per atomic mass units in the gas, $w \approx 5$ is the increase in the angular momentum loss rate due to relativistic effects (Miller & Lamb 1996), and \mathcal{E} is a function of photon energy and contains corrections for Coulomb scattering (Blumenthal 1974). Substituting equation (5) into equation (4) and integrating gives the time for matter to spiral from a radius r_0 to the stellar surface at r_* :

$$t_{\text{PR}} = \frac{\pi mc^2 (r_0^2 - r_*^2)}{\sigma_T L \zeta w \mathcal{E}}, \quad (6)$$

where m is the mass of the scattering particle in the accretion flow.

During the 4U 1820–30 superburst the illuminating spectrum was a blackbody with a peak temperature of $kT \approx 2.9 \text{ keV}$ (Strohmayer & Brown 2002). Since the vast majority of the illuminating photons have energies far above the ionization energy of helium (54.4 eV), $\zeta = 0.5$. Blumenthal (1974) shows in his equation (29) a limiting expression for \mathcal{E} in the case of a blackbody spectrum with $kT \ll mc^2$. Using this equation with $kT = 2.9 \text{ keV}$ gives $\mathcal{E} = 0.91$. The radius expansion phase observed early on in the superburst implies the peak luminosity was $\sim L_{\text{Edd}}$, which we will take to be $2.7 \times 10^{38} \text{ ergs s}^{-1}$ (§ 2). Collecting all the above results and scaling the disk radii to gravitational radii r_g gives a new expression for the time for matter to drain onto the neutron star due to Poynting-Robertson drag:

$$t_{\text{PR}} = 2 \times 10^{-6} \left(\frac{M}{1.4 M_{\odot}} \right)^2 \left(\frac{L}{L_{\text{Edd}}} \right)^{-1} \left[\left(\frac{r_0}{r_g} \right)^2 - \left(\frac{r_*}{r_g} \right)^2 \right] \text{ s}. \quad (7)$$

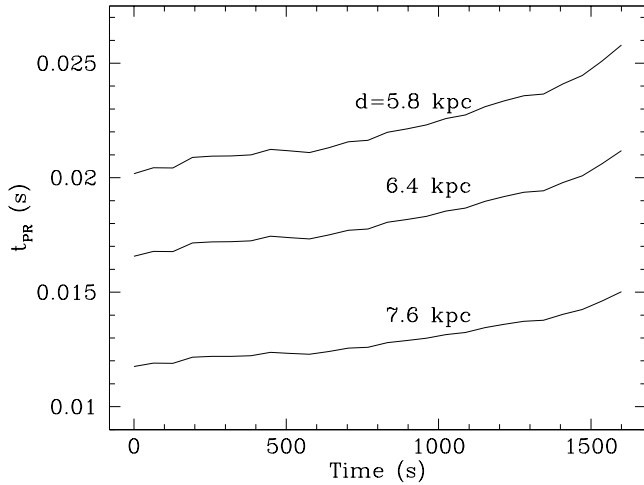


FIG. 4.—Timescale for matter to drain onto the neutron star via Poynting-Robertson drag during the initial ~ 1600 s of the 4U 1820–30 superburst. As the timescale is directly related to the luminosity, three lines are plotted for different estimates of the distance to the system. The luminosity was calculated as described in the caption to Fig. 1. In all three cases, t_{PR} is much less than 1 s.

Figure 4 plots the predicted time for matter to spiral down from $100r_g$ to the stellar surface at $\sim 5r_g$ during the first ~ 1600 s of the 4U 1820–30 superburst. The values of L/L_{Edd} were taken from Figure 1, and we show results for the different distance estimates to 4U 1820–30. For any distance, the Poynting-Robertson timescale is very small compared to the results of the spectral modeling, which showed an evolution in the reflecting region over 500–1000 s. However, equation (7) ignores processes such as outflows pushed by the radiation field (§ 3.1), viscous coupling of the gas, and radiative transfer effects that will randomize the radiation field in the optically thick disk material. All of these will slow down the infall rate onto the star, but it is unclear whether the timescale can be increased by the 4 orders of magnitude needed to bring it in line with the observed behavior. Poynting-Robertson drag also suffers from the same dependence on the incident flux as the radiative winds in § 3.1. In contrast, the X-ray reflection results show that the disk response was not dominated by the illuminating flux but rather by the spectral shape (Ballantyne & Strohmayer 2004).

Nevertheless, there are indications in the data that the Poynting-Robertson effect may be ongoing and affecting the disk structure. Ballantyne & Strohmayer (2004) found that late in the burst decay phase, the inner radius of the disk (as judged by the reflection features) was relatively steady between $10r_g$ and $20r_g$, much farther out than the innermost stable circular orbit of $\sim 6r_g$. At this point, the illuminating spectrum was cool and the observed flux was about 10 times lower than at the peak. It may be that at these low flux values, Poynting-Robertson is increasing the accretion rate at radii $\lesssim 10r_g$, thereby lowering the surface density and suppressing reflection features.

5. LOCAL CHANGES IN DISK STRUCTURE

The large X-ray flux released during a superburst or type I X-ray burst will significantly heat the surface of the surrounding accretion disk. In this section we consider how the disk may respond to this heating.³

³ This was discussed briefly by Ballantyne & Strohmayer (2004) but is presented more fully here. Values derived here supersede the earlier ones.

For a Thomson-thin plasma dominated by photoionization, the maximum equilibrium temperature obtainable (although free-free cooling will somewhat reduce the maximum temperature) is the Compton temperature kT_C ,

$$4kT_C \int_{E_1}^{E_2} u_E dE = \int_{E_1}^{E_2} u_E E dE, \quad (8)$$

where Compton heating is balanced by Compton cooling. In the above expression u_E is the spectral energy density of the radiation, and E is photon energy. For the case of a blackbody spectrum produced by a burst on a neutron star, $u_E \propto E^3/(e^{E/kT} - 1)$ and $kT_C \approx kT$. In response to this increased temperature, the surface layers of the disk will have to adjust in order to maintain hydrostatic balance. The timescale of this readjustment is of the order of the dynamical time $t_z \sim t_\phi \sim 4 \times 10^{-6} (M/M_\odot)(R/r_g)^{3/2}$ s (Frank et al. 2002), which is essentially instantaneous at distances close to the neutron star. The new hydrostatic configuration will evolve to a larger disk scale height $H \propto c_s r^{3/2} \propto T^{1/2} r^{3/2}$, implying that the disk thickness will closely track the hardness of the burst spectrum. This is interesting because the 4U 1820–30 X-ray reflection results show a correlation with the temperature of the incident power law. Using standard theory (Shakura & Sunyaev 1973), the maximum accretion disk temperature for 4U 1820–30 is $0.51(d/6.4 \text{ kpc})^{-1}$ keV. The temperature of the blackbody spectrum peaked at ~ 2.9 keV (Strohmayer & Brown 2002), so that at this point the scale height of the disk atmosphere may have increased by a factor of at least 2.

Significant changes to the surface density due to internal viscosity mechanisms occur on the viscous timescale, t_{visc} , which is typically much longer than the dynamical time (Frank et al. 2002). For the gas pressure supported, electron scattering dominated disk described in § 3.1.1,

$$t_{\text{visc}} \sim 4.9 \times 10^{24} [0.2(1+X)]^{-1/5} (\mu m_p)^{4/5} \alpha^{-4/5} \times \left(\frac{M}{M_\odot}\right)^{8/5} \dot{M}^{-2/5} \left(\frac{R}{r_g}\right)^{7/5} J(R)^{-2/5} \text{ s}, \quad (9)$$

where the symbols are the same as in equation (3). Substituting values appropriate for 4U 1820–30 (see §§ 2 and 3.1.1), we obtain

$$t_{\text{visc}} \sim 0.22 \alpha^{-4/5} \left(\frac{M}{1.4 M_\odot}\right)^{8/5} \left(\frac{\dot{M}}{1.1 \times 10^{17} \text{ g s}^{-1}}\right)^{-2/5} \times \left(\frac{d}{6.4 \text{ kpc}}\right)^{-4/5} \left(\frac{R}{r_g}\right)^{7/5} J(R)^{-2/5} \text{ s}. \quad (10)$$

Figure 5 plots t_{visc} as a function of radius, assuming three different values of the viscosity parameter α and a distance of 6.4 kpc (the other distances do not greatly affect the results). The viscous timescales predicted for $\alpha \sim 0.1$ –0.2 are in the appropriate range to potentially explain the evolution of the X-ray reflection features between $20r_g$ and $100r_g$. The effective α can, of course, vary from region to region in the disk and from time to time (Hawley & Krolik 2001; Armitage et al. 2001; Hawley 2001), so this should be considered an average value.

The viscous time can also be written as $t_{\text{visc}} \sim \alpha^{-1} (H/R)^{-2} t_\phi$, which illustrates an inverse dependence on the disk scale height. The estimates of t_{visc} from equation (10) assumed an unaltered scale height. As noted above, X-ray heating could increase H by ~ 2 , thereby reducing the viscous time by ~ 4 . If α is now assumed to be ~ 0.025 –0.05, then this would maintain roughly the same t_{visc} as those plotted in Figure 5. As t_{visc} is changing as the

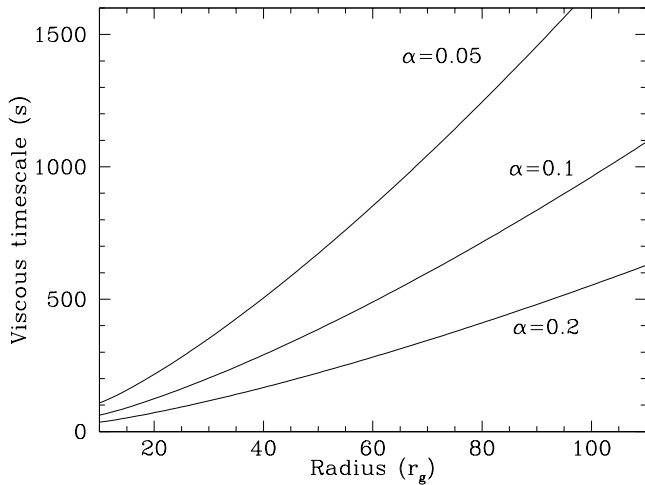


FIG. 5.—Viscous timescale for a gas pressure supported disk with electron scattering opacity as a function of disk radius. The three curves denote different values of the Shakura-Sunyaev viscosity parameter. A distance to 4U 1820–30 of 6.4 kpc was assumed, although use of the other two distances do not significantly change the results. The curves were calculated with eq. (10) and thus assume an unaltered scale height H .

gas is being heated, it may be difficult to obtain an accurate estimate of α .

Since equation (10) predicts approximately the correct timescale for the observed evolution in 4U 1820–30, it strongly suggests that the superburst caused a significant change in the disk structure, which is then propagated on a viscous time. X-ray heating will cause the disk scale height to increase, but this will occur locally very quickly. We hypothesize that the sudden, intense, and relatively long-lasting X-ray illumination from a superburst can affect the angular momentum transport mechanism of the disk.

6. DISCUSSION

6.1. The Response of the Accretion Disk around 4U 1820–30

This paper has discussed mechanisms that could influence the structure or dynamics of an accretion disk around a neutron star undergoing a type I X-ray burst or a superburst. The motivation was to determine an explanation for the apparent evolution of the accretion disk around 4U 1820–30 during a superburst (Ballantyne & Strohmayer 2004). Here we will look at the different possibilities identified above and determine their effectiveness in explaining the observations.

A radiatively driven wind off the accretion disk is an effective means to remove mass from the inner regions of the disk. However, this scenario faces several difficulties when confronted with the data. First, the outflow can only be driven by super-Eddington luminosities. As mentioned in § 2, X-ray bursts are not expected to greatly exceed L_{Edd} , and so the superburst would have only reached that luminosity for a very short time at the initial stage of the explosion. Ballantyne & Strohmayer (2004) found that the X-ray-reflecting region drastically changed ~ 500 s into the burst, when the luminosity would have been sub-Eddington. Second, the mass outflow rates predicted by the numerical wind calculations are too small to remove the inner disk (assuming it is a Shukura-Sunyaev disk) unless it subtends a significant fraction of the sky as seen from the X-ray source. Furthermore, the accretion rate through the disk is of the same order or even greater than the predicted outflow rates and thus increases the difficulty in removing the inner disk.

On the other hand, it may not be necessary to completely excavate the inner disk in order to remove the reflection features. All that is required is to replace the optically thick, efficiently reflecting disk with something that is a poor reflector. If a wind is blown off the disk, then it may obscure the surface from the X-rays and thereby destroy the reflection features. The longer observed timescale may be related to this more inefficient evaporation of the disk. More-detailed simulations are required to test this idea.

In § 4 we found that Poynting-Robertson drag is an efficient mechanism to remove angular momentum from the gas. However, the predicted infall timescale is so rapid that the superburst would drain the entire accretion disk onto the star in only a few seconds. Clearly, the simple analytic estimate employed in § 4 is not applicable to the case of optically thick accretion disks. One important issue with the analysis is the single particle assumption in equation (7). If the illuminated gas on the disk is significantly coupled by the viscous stresses (e.g., magnetically) to other areas in the disk, then the mass and cross section of this larger, more massive parcel of gas would replace the single particle in equation (7). The details of this coupling would obviously depend on the viscous physics within the accretion disk but could produce a mechanism to reduce the angular momentum loss rate in this material. A full radiation hydrodynamics simulation that included radiative transfer would be needed to completely elucidate the effects of radiation drag on the disk material. It seems likely, therefore, that radiation drag will only be important for the very innermost regions of the accretion flow (as concentrated on by Miller & Lamb 1996). The high luminosity of the burst will very quickly reduce the angular momentum from this material and increase the local accretion rate. We would expect the decay timescale to increase dramatically beyond this small range of radii. This is a potential explanation for why the inner radius of the reflecting region never falls below $\sim 10r_g$ (see also § 6.2 below).

The final mechanism considered in the paper involved neither outflow nor inflow (although it seems likely that both are occurring at some level) but rather a change in disk structure or surface density due to X-ray heating. This scenario is the easiest to explain the correlations seen in the X-ray data, as it predicts a strong dependence on the blackbody temperature (rather than the flux), and the viscous timescale is of the right order (with $\alpha \sim 0.03$ – 0.2) to account for the trends seen in the reflections fits. However, it is the hardest to justify theoretically, because the X-ray heating would change the local disk structure on a dynamical time, much faster than the viscous time. We suggest, therefore, that the intense and long-lasting heating does have a large impact on the disk transport mechanisms, which will change on the appropriate timescale. If the surface density drops globally over the inner accretion disk, because of the material being “puffed up” by X-ray heating, then it could easily become an inefficient reflector. Unfortunately, to truly determine whether this mechanism is the correct explanation and to determine its importance relative to the inflow and outflow scenarios described above, a full numerical simulation that encompasses all the relevant physics will need to be performed. This is planned for future work.

Of course, there is the possibility that the spectral features identified by Strohmayer & Brown (2002) are not due to reflection at all. Shaposhnikov & Titarchuk (2002) argue that since the disk will be heated very quickly to the blackbody temperature by the burst, all the heavy metals will be entirely ionized and unable to produce reflection features. These authors propose that the Fe $K\alpha$ line and edge are formed in an outflow

from the stellar surface (Titarchuk & Shrader 2005). While it is possible that spectral features may form in an outflow (although it would be unusual to find a large column of heavy metals close to the surface of a neutron star; Bildsten et al. 1992, 2003), it is not clear that the disk will be entirely ionized by the superburst. Numerical simulations of accretion disks subject to the magnetorotational instability consistently find that the gas is inhomogeneous and clumpy because of turbulence (e.g., Hawley & Krolik 2001). These density inhomogeneities may enhance the line emission in the X-ray reflection spectrum (Ballantyne et al. 2004).

The spectral fitting by Ballantyne & Strohmayer (2004) measured the ionization parameter $\xi = 4\pi F_X/n_{\text{He}}$ of the reflecting region on the disk. Shakura-Sunyaev disk theory can be used to estimate ξ and determine whether the disk is expected to be completely overionized. Writing $n_{\text{He}} = \Sigma/m_{\text{He}}H$ and the X-ray flux as $F_X = L/4\pi R^2$, we obtain

$$\xi \approx \frac{Lm_{\text{He}}H}{R^2\Sigma}. \quad (11)$$

The scale height H for a gas pressure dominated disk with electron scattering opacity is

$$H = 1.4 \times 10^{-10} (\mu m_p)^{-2/5} [0.2(1+X)]^{1/10} \alpha^{-1/10} \times \left(\frac{M}{M_\odot}\right)^{7/10} \left(\frac{R}{r_g}\right)^{21/20} \dot{M}^{1/5} J(R)^{1/5} \text{ cm}. \quad (12)$$

Using this expression, equation (3), $X \approx 0$, and $\mu \approx 1.3$, we now obtain

$$\xi \approx 1500\alpha^{7/10} \left(\frac{L}{L_{\text{Edd}}}\right) \left(\frac{M}{1.4 M_\odot}\right)^{-9/10} \left(\frac{R}{r_g}\right)^{-7/20} \times \left(\frac{\dot{M}}{1.1 \times 10^{17} \text{ g s}^{-1}}\right)^{-2/5} \left(\frac{d}{6.4 \text{ kpc}}\right)^{-4/5} J(R)^{-2/5} \text{ ergs cm s}^{-1}. \quad (13)$$

Figure 6 plots the predicted ξ at the radius measured by the spectral fitting of Ballantyne & Strohmayer (2004), assuming it is illuminated by the luminosity plotted in Figure 1. Following the results of § 5, we have also assumed $\alpha = 0.1$. Overplotted on the figure are the measured values of the ionization parameter as inferred from the spectral fitting.

In contrast to the expectations of Shaposhnikov & Titarchuk (2002), the disk does not have to be overionized by the burst. Rather, Figure 6 shows that the predicted ξ is generally much smaller than the measured one, especially near the beginning of the superburst. A simple way to bring the theoretical prediction of ξ in line with the measured one is to have a variable surface density that is ~ 40 times smaller over the first ~ 1000 s but then becomes only ~ 8 times smaller a couple of hours later, as the burst is decaying. Of course, increasing the scale height also results in a larger ξ . The exact behavior of how the surface density would evolve as a function of radius and burst luminosity would have to be calculated with a numerical simulation. Finally, Figure 6 shows that the predicted ξ follows the same trend as those inferred from the spectral fitting, supporting the ionized reflection interpretation of the observed spectral features.

There are additional dynamical effects that arise in bursting systems that could affect the accretion flow. For example, while models of PRE bursts show that the luminosity from the photosphere will barely exceed the Eddington limit, they also indicate that winds will be driven from the surface of the star

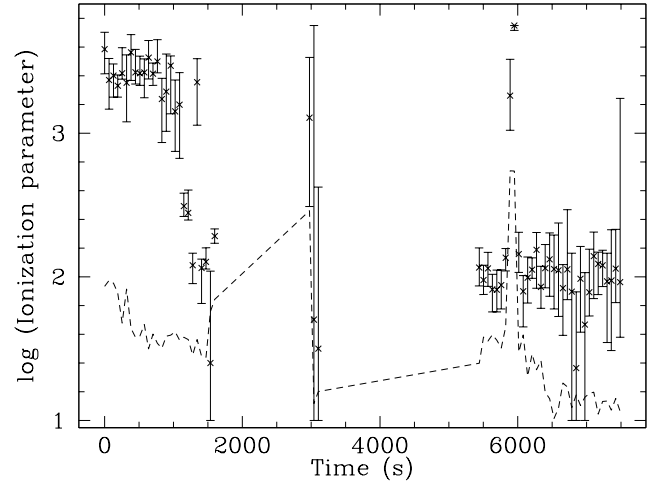


FIG. 6.—Dashed line plots the predicted value of the disk ionization parameter from eq. (13) during the 4U 1820–30 superburst. The points are the best-fit values from the reflection modeling of Ballantyne & Strohmayer (2004). A distance of 6.4 kpc and $\alpha = 0.1$ was assumed for the theoretical estimate. In order to bring the prediction in line with the observations, the surface density must be decreased by about a factor of 40 at the beginning of the burst, but this decreases to ~ 8 at later times.

(Ebisuzaki et al. 1983; Kato 1983, 1985; Quinn & Paczyński 1985; Paczyński & Anderson 1986; Paczyński & Prószyński 1986; Joss & Melia 1987). Thus, while the burst radiation may not blow away the disk, there may be a mechanical interaction between the stellar wind and the accretion flow. However, the outflows generally carry very little kinetic energy compared to the radiative energy released in the burst, so any mechanical interaction is unlikely to be significant. Secondly, the X-ray-heated gas on the disk surface will want to move to larger radii because of the gas pressure gradient as well as radiation pressure. This tendency to rotate at larger radii will be counteracted by viscous transport within the hot gas and radiative drag. Therefore, there may be some interesting dynamics within the disk as a response to X-ray bursts.

6.2. Disk Truncation and Magnetic Effects

Modeling of the reflection features in the spectra of the 4U 1820–30 superburst showed that there was little to no reflection within a radius of $\sim 15r_g$ (Ballantyne & Strohmayer 2004), much larger than the innermost stable circular orbit at $6r_g$. One explanation for this apparently truncated accretion flow is locally enhanced accretion due to Poynting-Robertson drag (§ 4). Alternatively, this radius may correspond to the magnetospheric radius, R_m , for which the magnetic pressure from the neutron star's magnetic field is equal to the gas ram pressure in the accretion flow. Within R_m the dynamics of the accreting gas is dominated by the magnetic field, and therefore the disk may be easily disrupted into a configuration that is unlikely to produce reflection features.

The magnetospheric radius is (Ghosh & Lamb 1978, 1979)

$$\left(\frac{R_M}{r_g}\right) \approx 1.3 \times 10^{-9} \left(\frac{M}{M_\odot}\right)^{-8/7} \dot{M}^{-2/7} \mu_m^{4/7}, \quad (14)$$

where μ_m is the magnetic moment of the stellar field (assuming dipole geometry). Substituting $M = 1.4 M_\odot$ and $\dot{M} \approx 1.1 \times 10^{17} (d/6.4 \text{ kpc})^2 \text{ g s}^{-1}$ and taking $r_m \approx 15r_g$, we find that $\mu_m \approx 2.8 \times 10^{26} (d/6.4 \text{ kpc}) \text{ G cm}^3$, or $B \sim 3 \times 10^8 (d/6.4 \text{ kpc}) \text{ G}$. This is a reasonable field strength for a nonpulsating LMXB system (Psaltis & Chakrabarty 1999). In fact, almost all systems that

exhibit X-ray bursts, and LMXBs in general, do not show X-ray pulsations (Lewin et al. 1993), implying much weaker field strengths than pulsars (which have $B \sim 10^{12}$ G). Thus, it is possible that the lack of X-ray reflection from within $\sim 15r_g$ may be due to magnetic truncation.

6.3. Prospects for Future Observations

The superburst from 4U 1820–30 occurred when the system was being observed by the *Rossi X-Ray Timing Explorer* (*RXTE*). As a result, the sensitive narrowband instruments on board were able to pick up the reflection features and track their evolution as the burst evolved. So far only one other system has been as fortunate (4U 1636–53; Strohmayer & Markwardt 2002; Kuulkers et al. 2004). Superbursts are the ideal events for which to search for X-ray reflection features from the accretion disk, as they last for a number of hours. Moreover, because of this long timescale, the analyses presented in this paper predict that we are more likely to observe changes to the accretion disk during superbursts than during the much shorter type I X-ray bursts. The major difficulty is the unknown recurrence time of superbursts, which can vary over a number of years depending on the composition of the accreted material (Cumming 2003). Nevertheless, we suggest that rapid X-ray follow-up of superbursts would be an important secondary science objective for the *Swift* mission. Detecting reflection features from a variety of systems with different orbital and spin periods, magnetic field strengths and evolutionary paths would allow examination of the accretion process over a wide parameter space.

As the overall geometry is the same and the light travel time is much shorter than the burst duration, X-ray reflection features should be produced in type I bursts as well. The difficulty will be detecting them with sensitive enough instruments to do time-averaged spectral analysis let alone time-resolved studies. However, type I events are much more common than superbursts, allowing repeatable experiments and tests of hypotheses. Sensitive spectral analysis of type I X-ray bursts would be an important objective for a future high-throughput observatory.

7. CONCLUSIONS

Type I X-ray bursts or superbursts on neutron stars produce a significant amount of energy ($\sim 10^{39}$ or $\sim 10^{42}$ ergs, respec-

tively) in a short amount of time. In this paper, we have discussed how this energy, in the form of an X-ray flux, would affect the surrounding accretion flow. The goal was to elucidate the meaning behind the apparent evolution of the accretion disk uncovered by Ballantyne & Strohmayer (2004) in their analysis of X-ray reflection features observed during the 4U 1820–30 superburst.

Three separate physical processes were considered. The first, radiatively driven winds, was predicted to exist for $L/L_{\text{Edd}} \gtrsim 1$, but, for a thin accretion disk, the outflow rate was less than the accretion rate, so this effect may not produce a large change to the accretion flow. In contrast, Poynting-Robertson drag was predicted to be too efficient and would have removed the inner accretion disk in less than a second. This was the result of using a too simple description of the problem, but Poynting-Robertson may be dominant very close to the central star. The final process considered was a change in surface density due to X-ray heating. This successfully reproduced the observed timescale for a Shakura-Sunyaev viscosity parameter of $\alpha \sim 0.03$ – 0.2 but requires the *Ansatz* that the X-ray heating will result in significant changes to the surface density of the disk that would propagate on a viscous time. Our conclusion is that, while the X-ray heating may dominate the explanation of the observations, all three processes will be ongoing during a superburst, and numerical simulations are required to fully understand the response of the accretion disk to such large explosions.

Finally, we emphasize that future rapid follow-up observations of X-ray bursts (both super and otherwise) will be vital in the progress of this problem. X-ray reflection features should be common in these systems and any observed changes are likely to correspond to changes in the accretion flow. Further examples are needed to test the ideas presented here as well as provide constraints on accretion theory.

The authors thank C. Matzner and T. Strohmayer for useful discussions and comments and the anonymous referee for suggestions that improved the presentation of the paper. This research was supported by the Natural Sciences and Engineering Research Council of Canada.

REFERENCES

- Armitage, P. J., Reynolds, C. S., & Chiang, J. 2001, *ApJ*, 548, 868
 Bailyn, C. D., & Grindlay, J. E. 1987, *ApJ*, 316, L25
 Ballantyne, D. R., & Strohmayer, T. E. 2004, *ApJ*, 602, L105
 Ballantyne, D. R., Turner, N. J., & Blaes, O. M. 2004, *ApJ*, 603, 436
 Bildsten, L. 1998, in *The Many Faces of Neutron Stars*, ed. R. Buccheri, J. van Paradijs, & M. A. Alpar (Dordrecht: Kluwer), 419
 Bildsten, L., Chang, P., & Paerels, F. 2003, *ApJ*, 591, L29
 Bildsten, L., Salpeter, E. E., & Wasserman, I. 1992, *ApJ*, 384, 143
 Blumenthal, G. R. 1974, *ApJ*, 188, 121
 Cornelisse, R., Heise, J., Kuulkers, E., Verbunt, F., & in 't Zand, J. J. M. 2000, *A&A*, 357, L21
 Cumming, A. 2003, *ApJ*, 595, 1077
 ———. 2004, *Nucl. Phys. B (Proc. Suppl.)*, 132, 435
 Cumming, A., & Bildsten, L. 2001, *ApJ*, 559, L127
 Ebisuzaki, T., Hanawa, T., & Sugimoto, D. 1983, *PASJ*, 35, 17
 Everett, J. E., & Ballantyne, D. R. 2004, *ApJ*, 615, L13
 Ferland, G. J. 2002, *Hazy*, a Brief Introduction to CLOUDY, University of Kentucky Department of Physics and Astronomy Internal Report (Lexington: Univ. Kentucky)
 Font, A. S., McCarthy, I. G., Johnstone, D., & Ballantyne, D. R. 2004, *ApJ*, 607, 890
 Frank, J., King, A., & Raine, D. J. 2002, *Accretion Power in Astrophysics* (3rd ed.; Cambridge: Cambridge Univ. Press)
 Ghosh, P., & Lamb, F. K. 1978, *ApJ*, 223, L83
 ———. 1979, *ApJ*, 232, 259
 Grindlay, J., Gursky, H., Schnopper, H., Parsignault, D., Heise, J., Brinkman, A. L., & Schrijver, J. 1976, *ApJ*, 205, L127
 Haberl, F., Stella, L., White, N. E., Gottwald, M., & Priedhorsky, W. C. 1987, *ApJ*, 314, 266
 Hawley, J. F. 2001, *ApJ*, 554, 534
 Hawley, J. F., & Krolik, J. H. 2001, *ApJ*, 548, 348
 Joss, P. C., & Melia, F. 1987, *ApJ*, 312, 700
 Kato, M. 1983, *PASJ*, 35, 33
 ———. 1985, *PASJ*, 37, 19
 Kuulkers, E. 2004, *Nucl. Phys. B (Proc. Suppl.)*, 132, 466
 Kuulkers, E., den Hartog, P. R., in 't Zand, J. J. M., Verbunt, F. W. M., Harris, W. E., & Cocchi, M. 2003, *A&A*, 399, 663
 Kuulkers, E., in 't Zand, J., Homan, J., van Straaten, S., Altamirano, D., & van der Klis, M. 2004, in *X-ray Timing 2003: Rossi and Beyond*, ed. P. Kaaret, F. K. Lamb, & J. H. Swank (New York: AIP), 257
 Lewin, W. H. G., Vacca, W. D., & Basinska, E. M. 1984, *ApJ*, 277, L57
 Lewin, W. H. G., van Paradijs, J., & Taam, R. E. 1993, *Space Sci. Rev.*, 62, 223
 ———. 1995, in *X-Ray Binaries*, ed. W. H. G. Lewin, J. van Paradijs, & E. P. J. van den Heuvel (Cambridge: Cambridge Univ. Press), 175
 Miller, M. C., & Lamb, F. K. 1993, *ApJ*, 413, L43
 ———. 1996, *ApJ*, 470, 1033
 Paczyński, B., & Anderson, N. 1986, *ApJ*, 302, 1
 Paczyński, B., & Prószyński, M. 1986, *ApJ*, 302, 519
 Pandey, G., Kameswara Rao, N., Lambert, D. L., Jeffrey, C. S., & Asplund, M. 2001, *MNRAS*, 324, 937

- Poynting, J. H. 1903, *Philos. Trans. R. Soc. London A*, 202, 525
- Psaltis, D., & Chakrabarty, D. 1999, *ApJ*, 521, 332
- Quinn, T., & Paczyński, B. 1985, *ApJ*, 289, 634
- Rappaport, S., Nelson, L. A., Ma, C. P., & Joss, P. C. 1987, *ApJ*, 322, 842
- Rasio, F. A., Pfahl, E. D., & Rappaport, S. 2000, *ApJ*, 532, L47
- Rich, R. M., Mignani, D., & Liebert, J. 1993, *ApJ*, 406, 489
- Robertson, H. P. 1937, *MNRAS*, 97, 423
- Shakura, N. I., & Sunyaev, R. A. 1973, *A&A*, 24, 337
- Shaposhnikov, M., & Titarchuk, L. 2002, *ApJ*, 567, 1077
- . 2004, *ApJ*, 606, L57
- Stella, L., Priedhorsky, W., & White, N. E. 1987, *ApJ*, 312, L17
- Strohmayer, T. E., & Bildsten, L. 2005, in *Compact Stellar X-ray Sources*, ed. W. H. G. Lewin & M. van der Klis (Cambridge: Cambridge Univ. Press), in press (astro-ph/0301544)
- Strohmayer, T. E., & Brown, E. F. 2002, *ApJ*, 566, 1045
- Strohmayer, T. E., & Markwardt, C. B. 2002, *ApJ*, 577, 337
- Svensson, R., & Zdziarski, A. A. 1994, *ApJ*, 436, 599
- Titarchuk, L., & Shrader, C. 2005, *ApJ*, 623, 362
- Vacca, W. D., Lewin, W. H. G., & van Paradijs, J. 1986, *MNRAS*, 220, 339
- Verbunt, F. 1987, *ApJ*, 312, L23
- Walker, M. A. 1992, *ApJ*, 385, 642
- Walker, M. A., & Mészáros, P. 1989, *ApJ*, 346, 844
- Zhang, W., Smale, A. P., Strohmayer, T. E., & Swank, J. H. 1998, *ApJ*, 500, L171